# Potential environmental impact of bromoform from Asparagopsis farming in Australia

Yue Jia[1, a], Birgit Quack[2*], Robert D. Kinley[3], Ignacio Pisso[4], Susann Tegtmeier[1]

[1] Institute of Space and Atmospheric Studies, University of Saskatchewan, Saskatoon, Canada

[2] GEOMAR Helmholtz Centre for Ocean Research Kiel, Kiel, Germany

[3] Commonwealth Scientific and Industrial Research Organisation (CSIRO), Agriculture and Food, Townsville, QLD, Australia

[4] Norwegian Institute for Air Research (NILU), Kjeller, Norway

[a] *now at*: Cooperative Institute for Research in Environmental Sciences (CIRES), University of Colorado Boulder, Boulder, CO, USA.

*Corresponding to*: B. Quack (bquack@geomar.de)

**Abstract**

To mitigate the rumen enteric methane ($CH_4$) produced by ruminant livestock, *Asparagopsis taxiformis* is proposed as an additive to ruminant feed. During the cultivation of *Asparagopsis taxiformis* in the sea or in terrestrial based systems, this macroalgae, like most seaweeds and phytoplankton, produces a large amount of bromoform ($CHBr_3$), which contributes to ozone depletion once released into the atmosphere. In this study, we focus on the impact of $CHBr_3$ on the stratospheric ozone layer resulting from potential emissions from proposed *Asparagopsis* cultivation in Australia. The impact is assessed by weighting the emissions of $CHBr_3$ with its ozone depletion potential (ODP), which is traditionally defined for long-lived halocarbons but has been also applied to very short-lived substances (VSLSs). An annual yield of $\sim 3.5 \times 10^4$ Mg dry weight is required to meet the needs of 50% of the beef feedlot and dairy cattle in Australia. Our study shows that the intensity and impact of $CHBr_3$ emissions varies, depending on location and cultivation scenarios. Of the proposed locations, tropical farms near the Darwin region are associated with largest $CHBr_3$ ODP values. However, farming of Asparagopsis using either ocean or terrestrial cultivation systems at any of the proposed locations does not have potential to significantly impact the ozone layer. Even if all *Asparagopsis* farming was performed in Darwin, the $CHBr_3$ emitted into the atmosphere would amount to less than 0.02% of the global ODP-weighted emissions. The impact of remaining farming scenarios is also relatively small even if the intended annual yield in Darwin is scaled by a factor 30 to meet the global requirements, which will increase the global ODP-weighted emissions up to $\sim 0.5\%$

## 1. Introduction

Livestock is responsible for about 15% total anthropogenic greenhouse gas (GHG) emissions weighted by radiative forcing (Gerber et al., 2013), ranking it amongst the main contributors to climate change. The global demand for red meat and dairy is expected to increase >50% by 2050 compared to 2010 level, thus mitigation measures to reduce the GHG emissions from the global livestock industry are in high demand (Beauchemin et al., 2020). Total GHG emissions (e.g., $CH_4$) from ruminant livestock contribute about 18% of the total global carbon dioxide equivalent ($CO_2$-eq) inventory (Herrero and Thornton, 2013). With a global warming potential ~30 times higher than carbon dioxide ($CO_2$) and a much shorter lifetime (~10 years, IPCC, 2021), ruminant enteric $CH_4$ is an attractive and feasible target for global warming mitigation.

Enteric $CH_4$ from ruminant livestock is produced and released into the atmosphere through rumen microbial methanogenesis (Morgavi et al., 2010). Methanogenic archaea (methanogens) intercept substrate $CO_2$ and $H_2$ liberated during bacterial fermentation of feed materials (Kamra, 2005), and during this inefficient digestion process (Herrero and Thornton, 2013; Patra, 2012), methanogen metabolism leads to reductive $CH_4$ production and loss of feed energy as $CH_4$ emissions. To abate enteric methanogenesis, different strategies such as feeding management and antimethanogenic feed ingredients, have been proposed and assessed (e.g., Moate et al., 2016; Mayberry et al., 2019; Beauchemin et al., 2020). Some types of macroalgae have been demonstrated to mitigate production of $CH_4$ during *in vitro* and *in vivo* rumen fermentation significantly (Machado et al., 2014; Kinley and Fredeen 2015; Li et al., 2018; Kinley et al., 2020; Abbott et al., 2020). Among the different macroalgae species, Kinley et al. (2016a) concluded that the red algae *Asparagopsis* spp. showed the most potential for reducing $CH_4$ production. Kinley et al. (2016b) further demonstrated that forage with the addition of 2% *Asparagopsis taxiformis* could eliminate $CH_4$ production *in vitro* without negative effects on forage digestibility. In recent animal experiments, reduction of enteric $CH_4$ production by more than 98% was achieved with only 0.2% addition of freeze-dried and milled *Asparagopsis taxiformis* to the to the organic matter (OM) content of feedlot cattle feed (Kinley et al., 2020).

Halogenated, biologically active secondary metabolites are pivotal in the reduction of $CH_4$ induced by Asparagopsis (Abbott et al., 2020). Most of the reduction is ascribed to bromoform ($CHBr_3$) inhibition of the $CH_4$ biosynthetic pathway within methanogens (Machado et al., 2016). $CHBr_3$ as

74    a natural halogenated volatile organic compound originates from chemical and biological sources
75    including marine phytoplankton and macroalgae (Carpenter and Liss, 2000; Quack and Wallace,
76    2003). When emitted to the atmosphere, $CHBr_3$ has an atmospheric lifetime shorter than six months
77    and is often referred to as a very short-lived substance (VSLS). Once released into the atmosphere,
78    degraded halogenated VSLSs can catalytically destroy ozone in the troposphere and stratosphere,
79    thus drawing them considerable interest (Engel and Rigby et al., 2018; Zhang et al., 2020).
80    Bromoform is the dominant compound among bromine-containing VSLSs emissions, resulting
81    mostly from natural sources (Quack and Wallace, 2003) and to a lesser degree from anthropogenic
82    production (Maas et al., 2019; 2021). With an atmospheric lifetime of about 17 days (Carpenter
83    and Reimann et al., 2014), $CHBr_3$ can deliver bromine to the stratosphere under appropriate
84    conditions of emission strength and vertical transport (e.g., Aschmann et al., 2009; Liang et al.,
85    2010; Tegtmeier et al., 2015, 2020) and thus contribute to ozone depletion in the lower and middle
86    stratosphere (e.g., Yang et al., 2014; Sinnhuber and Meul, 2015). Global research on enabling
87    large-scale seaweed *Asparagopsis* farming is increasing (Black et al., 2021) as it appears to be one
88    of the most promising options as an antimethanogenic feed ingredient to achieve carbon neutrality
89    in the livestock sector within the next decade (Kinley et al., 2020; Roque et al., 2021). In
90    consequence, the environmental impact of $CHBr_3$ due to *Asparagopsis* farming also needs to be
91    explored and elucidated. In this study, only the impact on the stratosphere is considered.
92    The hypothesis was that large scale cultivation of *Asparagopsis* would not contribute significantly
93    to depletion of the ozone layer. The aim of this study was to assess the impact of anthropogenic
94    and natural processes that may contribute to $CHBr_3$ emissions inherent in large scale production
95    of *Asparagopisis spp.* and the subsequent impact of $CHBr_3$ release to the atmosphere by using
96    cultivation in Australia as the model. Specific objectives were to inform the industry, policy
97    makers, as well as the scientific community on: (i) the potential impact of $CHBr_3$ associated with
98    mass production of *Asparagopsis* on atmospheric halogen budgets and ozone depletion; (ii)
99    potential impacts relative to variability in regional climate, atmospheric conditions, and convection
100   trends with different potentials for transport of $CHBr_3$ to stratospheric ozone; (iii) the combined
101   $CHBr_3$ emissions potential of ocean and terrestrial based cultivation of *Asparagopsis* to supply
102   sufficient biomass for up to 50% of beef feedlot and dairy cattle in Australia; and (iv) extrapolation
103   of the impacts of production to requirements on a global scale.
104

## 2. Data and Method

The potential impact of $CHBr_3$ on the atmospheric bromine budget and stratospheric ozone depletion, associated with *Asparagopsis spp.* mass production was assessed for assumed annual yields and particular production scenarios of macroalgae in Australia. Terrestrial systems cultivation and open ocean cultivation under different harvest conditions, variations of seaweed yield and growth rates for various scenarios and locations were tested as described in the following subsections.

### 2.1 Cultivation Scenarios

The cultivation scenarios in this study assume that sufficient seaweed is grown to supply *Asparagopsis spp.* to 50% of the Australian herds of beef cattle in feedlots (100%: ~$1.0 \times 10^6$) and dairy cows (100%: ~$1.5 \times 10^6$). For an effective reduction of $CH_4$ production from ruminants, a ~0.4% addition of freeze-dried and milled *Asparagopsis taxiformis* to the daily feed dry matter intake (DMI) is required (Kinley et al., 2020). This results in daily feed additions of 38 g dry weight (DW) *Asparagopsis* per head of feedlot cattle and 94 g DW *Asparagopsis* per head of dairy cows. In total, the required annual yield amounts to ~$3.5 \times 10^4$ Mg DW *Asparagopsis* to supplement the feed of roughly 50% of the Australian feedlot cattle and Australian dairy cows. Assuming that fresh weight (FW) has a DW content of 15%, a total of ~$2.3 \times 10^5$ Mg FW *Asparagopsis* needs to be harvested every year.

For a global scenario, we make the functional assumptions that: (i) there would be adoption of 30% of the global feed base to be supplemented with *Asparagopsis* farmed in Australia to reduce ruminant $CH_4$ production worldwide; (ii) *Asparagopsis* would be adopted by 50% of Australia's feedlot and dairy industries; and (iii) this is approximately equivalent to 1% of the global feedlot and dairy herds for the purpose of both assumed magnitude of production and adoption relevant for calculations of supply and emissions. This export scenario requires for 30 times increased production compared to the Australian scenario if all the required *Aspargopsis* was to be cultivated in Australia and an annual harvest of ~1 Tg DW *Asparagopsis* would be needed from Australian waters.

For the future farm distributions in Australia, we assume that *Asparagopsis* will be cultivated in open ocean systems and terrestrial confinement systems (that may include, but not limited to, tanks,

136    raceways, and ponds) located near Geraldton, Triabunna, and Yamba (Figure 1). We assume that

137    one third of the required annual yield ($\sim 1.2 \times 10^4$ Mg DW) is grown near Triabunna (T), with 60%

138    in terrestrial systems and 40% in open ocean farms, one third is grown in terrestrial systems at

139    Yamba (Y), and the last third is grown in the open ocean in Geraldton (G). For comparison of the

140    environmental impact, we also adopt a tropical scenario where all farms with their total annual

141    yield of $\sim 3.5 \times 10^4$ Mg DW are assumed to be situated near Darwin.

142    The emissions of CHBr$_3$ from the macroalgae farms can be derived based on estimates of the

143    standing stock biomass. For any given farming scenario, the standing stock biomass $B_f$ (g DW) is

144    a function of time $t$ and can be calculated from the initial biomass $B_i$ (g DW) and the specific

145    growth rate $GR$ (%/day) according to Hung et al. (2009):

146
$$B_f(t) = B_i \cdot (1 + GR/100)^t \qquad\qquad (1)$$

147    Terrestrial systems and open ocean cultivation scenarios are assuming a fixed targeted annual

148    yield. For a given initial biomass and growth rate, the length and frequency of the growth periods

149    per year need to be chosen accordingly, to achieve the required final yield. Yong et al. (2013)

150    checked the reliability of different equations for seaweed growth rate determination by comparing

151    the daily seaweed weight cultivated under optimized growth condition, and the most reliable

152    relationship between initial and final weight leads to the form of Eq (1). We also applied several

153    growth rates from 1 to 10% to show the possible influence of this parameter on the overall

154    emissions of the algae. Average growth rates of *Asparagopsis* ranged from 7 to 13 %/day in

155    samples from tropical and sub-tropical Australia during short-term experiments (Mata et al., 2017).

156    We used a lower growth rate of 5% for our scenario to provide an upper estimate of potential

157    CHBr$_3$ emissions. Note that emissions decrease by 27% when using a growth rate of 7% as

158    demonstrated in section 3.1.

159    Figure 2 provides an example of the variations of standing stock of *Asparagopsis* for the farms of

160    Geraldton (all open ocean) and Yamba (all terrestrial systems) with a growth rate of 5% per day.

161    For the open ocean cultures, we assume a scenario of six harvests per year and 60 day growth

162    periods to obtain the annual yield (Battaglia, 2020; Elsom, 2020). For a sensitivity study, we

163    assume an alternative scenario based on the same initial biomass, but only one harvest per year.

164    As evident from Figure 2, the same annual yield can be achieved with one harvest per year if

165  applying an extended growth period of 96 days. For the tank cultures, a harvest every 5 days (73

166  harvests per year) is assumed as a realistic scenario (Battaglia, 2020; Elsom, 2020).
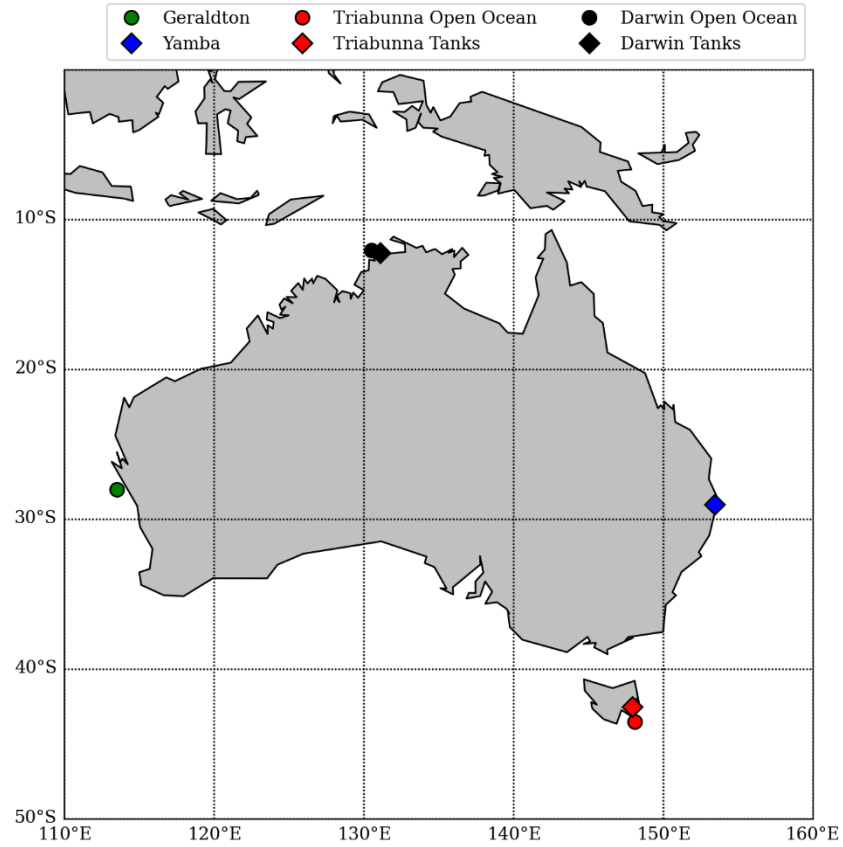
167
168  **Figure 1.** Locations of actual *Asparagopsis* farms in Geraldton, Triabunna, Yamba, and theoretical
169  farms in Darwin.
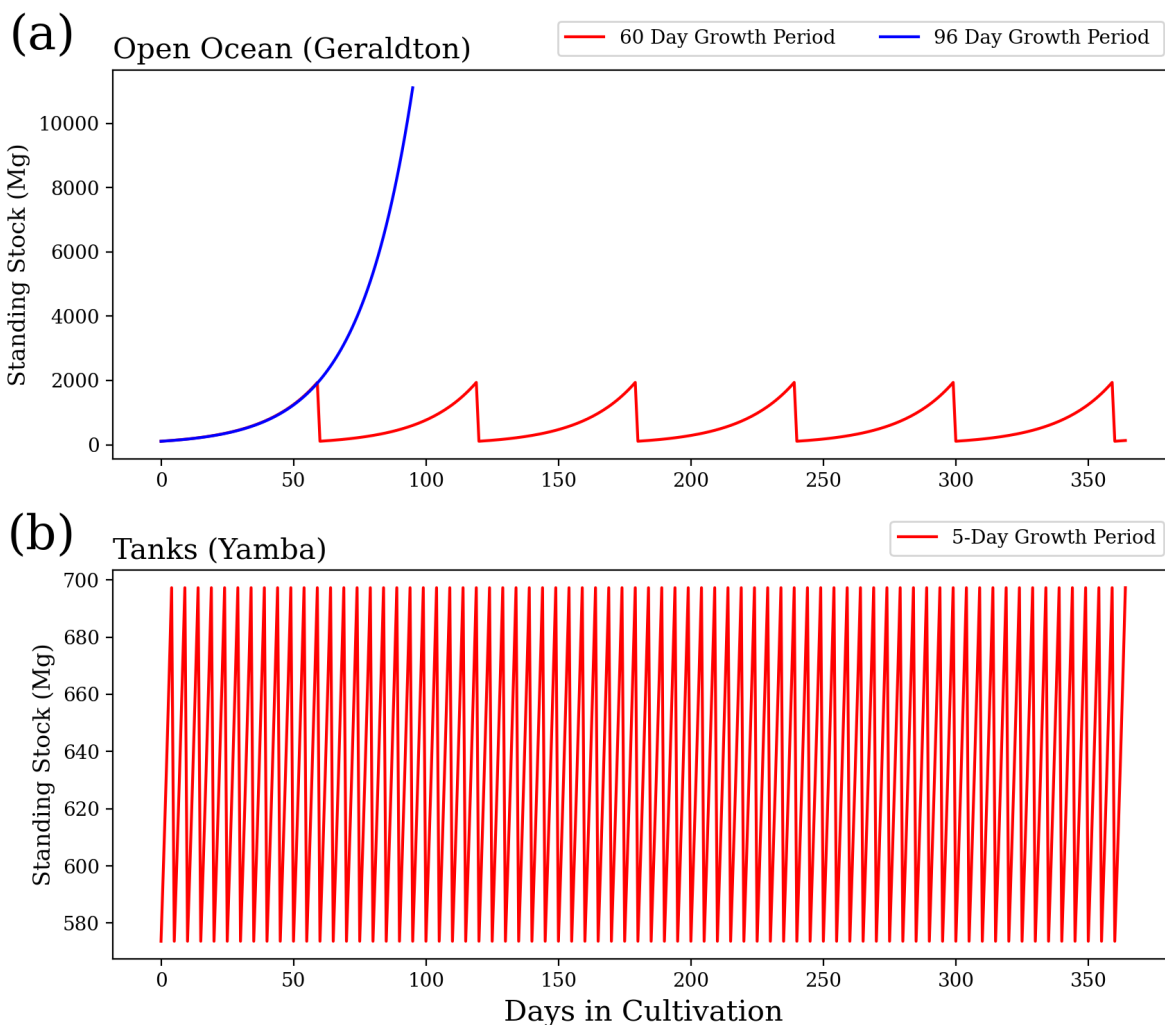
**Figure 2.** Standing stock biomass of *Asparagopsis* cultivation a) in the open ocean for a 60-day growth period and 96 day growth period and b) in terrestrial systems culture for a 5 day growth period. Each of the three scenarios will achieve an annual yield of ~$1.6 \times 10^4$ Mg DW.

### 2.2 *Asparagopsis* CHBr₃ release rates

Rates of the $CHBr_3$ content in *Asparagopsis* given in the literature range between 3.4 to 43 mg $CHBr_3$/g DW, with values around 10 mg $CHBr_3$/g DW appearing to be realistic in current cultivation (Burreson and Moore, 1976; Mata et al., 2012, 2017; Paul et al., 2006; Vucko et al., 2017). We assume that *Asparagopsis* strain selection cultivated for feed supplements will lead to high yielding $CHBr_3$ varieties thus we assume augmented $CHBr_3$ production with a mean content

182    of 21.7 mg CHBr$_3$/g DW (Magnusson et al., 2020) for this study.

183    Very few values on the CHBr$_3$ release from *Asparagopsis* have been reported in the literature. A
184    constant release of 1100 ng CHBr$_3$/g DW hr$^{-1}$ was measured for *Asparagopsis armata*
185    *tetrasporophyte*, which has a CHBr$_3$ content of 14.5 mg CHBr$_3$/g DW (Paul et al., 2006). We
186    assume a linear scaling between the CHBr$_3$ release rates and the content. Thus, a cultivated
187    *Asparagopsis* for which we assume 21.7 mg CHBr$_3$/g DW should release around 1646 ng CHBr$_3$/g
188    DW hr$^{-1}$, a rate which has been confirmed by Marshall et al. (1999). Therefore, for our calculations,
189    we assume a constant release of 1600 ng CHBr$_3$/g DW hr$^{-1}$ for farmed *Asparagopsis* with a CHBr$_3$
190    content of 21.7 mg CHBr$_3$/g DW. These content and release rates are higher than those for wild
191    stock algae (Leedham et al., 2013; Nightingale et al., 1995) as the farming aims at algae varieties
192    with high CHBr$_3$ yield. As available information on this topic is very sparse no variations of the
193    release rate with life-cycle stages, season, location, or other environmental parameters were used
194    in this study. Also, the two species *Asparagopsis armata* and *Asparagopsis taxiformis* were treated
195    the same way as *Asparagopsis spp.*, as variations in CHBr$_3$ content and release within or between
196    species are currently unknown (Mata et al., 2017) and more research on this topic is needed.

197
198    **2.3 Parameterization of CHBr$_3$ Emission**
199
200    The emissions of CHBr$_3$ from farmed macroalgae are a function of the standing stock biomass (in
201    g DW) and can be calculated with the constant release rate ($R_{CHBr_3}$) of 1600 ng CHBr$_3$/g DW hr$^{-1}$
202    multiplied with the standing stock. The total release of CHBr$_3$ ($E_{CHBr_3}$) over the complete growth
203    period of T days is given by the integral over the daily emissions from day 1 to day *T*:

204    $$E_{CHBr_3} = \int_0^T 24 \cdot B_i \cdot (1 + GR)^t \cdot R_{CHBr_3} dt = 24 \cdot B_i \cdot R_{CHBr_3} \cdot \frac{[(1+GR)^T - 1]}{ln\,(1+GR)} \qquad (2)$$

205    For our atmospheric impact studies we assume, that all CHBr$_3$ released from the algae is emitted
206    into the atmosphere at its location of production. An increasing seawater concentration of CHBr$_3$
207    shifts the equilibrium conditions between seawater and air towards the atmosphere, as CHBr$_3$
208    easily volatilizes to the atmosphere. Consequently, air-sea exchange acts as a relatively fast loss
209    process for CHBr$_3$ in surface water. Oceanic sinks can also impact CHBr$_3$, but act on relatively
210    long timescales. Degradation through halide substitution and hydrolysis results in the ocean sink
211    CHBr$_3$ half-life of 4.37 years (Hense and Quack, 2009). Thus, most of the CHBr$_3$ contained in

212 surface seawater is instantly outgassed into the atmosphere without oceanic loss processes, playing
213 a role as confirmed by the modelling study of Maas et al. (2021).

214 The air-sea exchange of CHBr₃ is expressed as the product of its transfer coefficient ($k_w$) and the
215 concentration gradient ($\Delta c$) (Eq. (3)). The gradient is computed between the water concentration
216 ($c_w$) and theoretical equilibrium water concentration ($c_{atm}/H$), where $c_{atm}$ is the atmospheric
217 concentration and $H$ is Henry's law constant (Moore et al., 1995a; Moore et al., 1995b).

218
$$F = k_w \cdot \Delta c = k_w \cdot (c_w - \frac{c_{atm}}{H}) \qquad (3)$$

219 The compound-specific transfer coefficient ($k$w) is determined using the air-sea gas exchange
220 parameterization of Nightingale et al. (2000) (Eq. (4))

221
$$k_w = k \cdot \sqrt{Sc}/660 \qquad (4)$$

222 The transfer coefficient $k$ is a function of the wind speed at 10 m height ($u_{10}$): $k = 0.2u_{10}^2 +$
223 $0.3u_{10}$, and the Schmidt number ($Sc$) is a function of sea surface temperature (SST) from Quack
224 and Wallace (2003), which is expressed as $Sc = 4662.8 - 319.45 \cdot SST + 9.9012 \cdot SST^2 +$
225 $0.1159 \cdot SST^3$.

226 In this study, we use the CHBr₃ sea-to-air flux climatology from Ziska et al. (2013) as marine
227 background emissions. The global emission scenario from Ziska et al. (2013) is a bottom-up
228 estimate of the oceanic CHBr₃ fluxes, generated from atmospheric and oceanic surface ship-borne
229 *in situ* measurements between 1979 to 2013. Due to the paucity of data, the 35 year mean gridded
230 data set was filled by interpolating and extrapolating the *in situ* measurement data. The oceanic
231 emissions were calculated with the transfer coefficient parameterization of Nightingale et al.
232 (2000) and 6-hourly meteorological data, which allow a temporal emission variability related to
233 wind and temperature.

234
235 **2.4 Emission Scenarios for FLEXPART Simulations**
236

237 To quantify the atmospheric impact of CHBr₃ emissions from macroalgae farming, the Lagrangian
238 particle dispersion model FLEXPART (Pisso et al., 2019) is used. FLEXPART has been evaluated
239 extensively in previous studies (e.g., Stohl et al., 1998; Stohl and Trickl, 1999). The model includes
240 moist convection and turbulence parameterizations in the atmospheric boundary layer and free
241 troposphere (Forster et al., 2007; Stohl and Thomson, 1999). The European Centre for Medium-
242 Range Weather Forecasts (ECMWF) reanalysis product ERA-Interim (Dee et al., 2011) with a

243 horizontal resolution of 1° x 1° and 60 vertical model levels is used for the meteorological input

244 fields, providing air temperature, winds, boundary layer height, specific humidity, as well as

245 convective and large-scale precipitation with a 3-hour temporal resolution.

246 We conduct FLEXPART simulations for year 2018 with different emission scenarios as explained

247 in the following and summarized in Table 1:

248 1.) Australian scenarios: $CHBr_3$ emissions from the *Asparagopsis* farming in Geraldton,

249 Triabunna, and Yamba are calculated for an overall annual yield of 34674 Mg DW according to

250 Equation 2. For the terrestrial systems, 5 day growth periods are assumed resulting in 73 harvests

251 per year. For the open ocean, the assumption of different growth periods results in three sub-

252 scenarios a) 6 times 60 day growth periods with the first period starting on January 1$^{st}$ (referred to

253 as GTY_O60), b) one 96 day growth period starting on January 1$^{st}$ (GTY_O96_Jan), and c) and

254 another starting on July 1$^{st}$ (GTY_O96_Jul).

255 For the last Australian scenario, we assume that all farms are located around Darwin in the

256 Northern Territory tropics with 6 times 60 day growth periods in the open ocean and 73 times 5

257 day growth periods in the terrestrial systems (Darwin_O60). While this is an unlikely scenario

258 according to current plans, it is useful to demonstrate the influence of potential farming locations

259 on their environmental impact.

260 2.) Global scenarios: Emissions from *Asparagopsis* farming in Geraldton, Triabunna, and Yamba

261 are estimated according to the annual yield, upscaled by a factor of 30 to global requirements.

262 amounting to $1.04\times10^6$ Mg DW. Growth periods and harvesting frequencies are set up in the same

263 way as for the Australian scenarios. Short names of the global scenarios are the same as for the

264 Australian scenarios with the additional label 30x.

265 3) Background scenario: Emission from Ziska et al. (2013) for the entire coastal region around

266 Australia defined as all 1°x1° grid cells directly neighbouring the coastline (Ziska_Coast).

267 4.) Extreme event scenarios: We assume extreme conditions where a hypothetical tropical cyclone

268 causes implausible release of all $CHBr_3$ from the macroalgae farm and water into the atmosphere.

269 We focus on the case study of Geraldton and the tropical cyclone Joyce, which occurred from 6-

270 13 January 2018 around western Australia. We base the amount of available macroalgae biomass

271 on the Australian scenario and assume that the entire $CHBr_3$ content of all *Asparagopsis* at this

272 location is released at once. The two scenarios defined here assume that the tropical cyclone occurs

273 at the end of the 60 day growth period (Geraldton_Ex60) resulting in the release of 41.8 Mg $CHBr_3$

274    (21.7 mg $CHBr_3$/g DW * 1926 Mg DW) or at the end of the 96 day growth period
275    (Geraldton_Ex96) resulting in the release of 250.8 Mg $CHBr_3$ (21.7 mg $CHBr_3$ /g DW* 11558 Mg
276    DW).

277    The daily model output is recorded for all simulations. For the extreme event, which assumes the
278    destruction of a farm (Geraldton-Ex), the 3 hourly output is recorded. For all simulations, except
279    the background scenario and extreme scenario, trajectories are released from four regions of the
280    size of: a) Geraldton (open ocean, 11558 ha): 0.1°x0.1°; b) Triabunna (open ocean, 4623 ha):
281    0.06°x0.06°; c) Triabunna (terrestrial systems, 126 ha): 0.01°x0.01°; and d) Yamba (terrestrial
282    systems, 210 ha): 0.01°x0.01°. For the tropical and extreme scenarios, trajectories are released
283    from the Darwin and Geraldton farms, respectively. For the background scenario Ziska_Coast,
284    trajectories are released from the 1.0°x1.0° grid along the Australian coastline. Note that it is not
285    reasonable to compute the Ziska emission on the locations of farming as some farms are terrestrial.
286    However, if we assume all the farms are Geraldton-like (i.e., all grown in the open ocean), the
287    Ziska emission in Geraldton, Yamba and Triabunna will be 843 Mg, 295 Mg, and 676 Mg,
288    respectively. The amount of released $CHBr_3$ is evenly distributed among the trajectories and is
289    depleted during the Lagrangian simulations according to the atmospheric half-life of 17 days (*e*-
290    folding lifetime of 24 days) (Hossaini et al., 2010; Montzka and Reimann et al., 2010; Engel and
291    Rigby et al., 2018).

292

293

294

295

296

Table 1. Detailed information on the scenarios set up for the atmospheric transport simulations with FLEXPART (Geraldton, Triubanna, and Yamba: GTY)

| Name | | Total Yield (Mg DW) | CHBr$_3$ Emissions (Mg) | Notes | Simulation Period |
|---|---|---|---|---|---|
| **Australian Scenarios** | GTY_O60 | Total: 34674 | Total: 27.3 | 6 harvests (every 60 days) in the open ocean; 73 harvests (every 5 days) in the terrestrial systems. | 01.01.2018 - 31.12.2018 2-month spin-up |
| | GTY_O96_Jan | Open Ocean: G: 11558 T: 4623 Y: - | Open Ocean: G: 9.10 T: 3.64 | 1 harvest (after 96 days) in open ocean; 73 harvests (every 5 days) in terrestrial systems. Growth in open ocean starts from 01.01.2018. | |
| | GTY_O96_Jul | Terrestrial systems: G: - T: 6935 Y: 11558 | Terrestrial systems: T: 5.46 Y: 9.10 | Same as GTY_O96_Jan but with growth in open ocean starting from 01.07.2018. | |
| | Darwin_O60 | Total: 34674 Open Ocean: Darwin: 16181 Terrestrial systems: Darwin:18493 | Total: 27.3 Open Ocean: Darwin: 12.7 Terrestrial systems: Darwin: 14.6 | Same as GTY_O60 but with farms near Darwin | |
| **Global Scenarios** | GTY_O60_30x | Total: 1040220 Open Ocean G: 346740 T: 138690 Y: - Terrestrial systems: G: - T: 208050 Y: 346740 | Total: 819 Open Ocean G: 273 T: 109.2 Terrestrial systems: T: 163.8 Y: 273 | Same as GTY_O60 but with initial biomass and areas 30 times larger. | |
| | GTY_O96_Jan_30x | | | Same as GTY_O96_Jan but with initial biomass and areas 30 times larger. | |
| | GTY_O96_Jul_30x | | | Same as GTY_O96_Jul but with initial biomass and areas 30 times larger. | |
| | Darwin_O60_30x | Total: 1040220 Open Ocean Darwin: 485430 | Total: 819 Open Ocean Darwin: 381 Terrestrial systems: Darwin: 438 | Same as Darwin_O60 but with initial biomass and areas 30 times larger. | |

| | | | | | |
|---|---|---|---|---|---|
| | | Terrestrial systems: Darwin: 554790 | | | |
| **Background Scenario** | Ziska_Coast | - | 3109 | CHBr$_3$ emission of the coastal region of Australia from Ziska et al. (2013) | |
| **Extreme Scenarios** | Geraldton_Ex60 | Open Ocean: G: 1926 | Open Ocean: G: 41.8 | Extreme event: CHBr$_3$ in Geraldton surface water before harvest is released due to tropical cyclone Joyce (07.01.2018 – 15.01.2018). Harvest period: 60 days. | 9.01.2018 – 9.02.2018 No spin-up |
| | Geraldton_Ex96 | Open Ocean: G: 11558 | Open Ocean: G: 250.8 | Same as Geraldton _Ex60 but with harvest period of 96 days | |

299

300

301   **2.5 Ozone Depletion Potential (ODP)**

302

303   The ozone depletion potential (ODP) is defined as the time-integrated potential destructive effect

304   of a substance to the ozone layer relative to that of the reference substance CFC-11 (CCl$_3$F) on a

305   mass emitted basis (Wuebbles, 1983). The ODP is a well-established and extensively used concept

306   traditionally defined for anthropogenic long-lived halocarbons. However, the concept has been

307   also applied to VSLSs (Brioude et al., 2010; Pisso et al., 2010): unlike the ODP for long-lived

308   halocarbons, which is one constant number, the ODP of a VSLS is a function of time and location

309   of the emissions. This variable number still describes the time-integrated ozone depletion resulting

310   from a CHBr$_3$ unit mass emission relative to the ozone depletion resulting from the same unit mass

311   emission of CFC-11. The ODP for VSLSs can be derived from chemistry-climate or chemistry

312   transport models simulating the changes of ozone due to certain compound (Claxton et al., 2019;

313   Zhang et al., 2020). The trajectory-derived ODP of VSLSs such as CHBr$_3$ is calculated as a

314   function of location and time of the potential emissions (Brioude et al., 2010; Pisso et al., 2010).

315   As for the traditional ODP concept, the time and space dependent ODP describes only the potential

316   of a compound but not its actual damaging effect to the ozone layer and is independent of the total

317   emissions. It is noteworthy that many VSLSs including CHBr$_3$ can impact ozone in the troposphere

318   and stratosphere. As ODPs are used to assess stratospheric ozone depletion only, the contribution

319   of VSLSs to tropospheric ozone destruction needs to be excluded when calculating their ODP

320   (Pisso et al., 2010; Zhang et al., 2020). The trajectory based ODP from Pisso et al. (2010) used in

321   this study considers only the impact of CHBr$_3$ on the stratospheric ozone instead of the ozone

column. The fraction of originally emitted VSLSs reaching the stratosphere depends strongly on the meteorological conditions. In particular, it shows a pronounced seasonality. Here we apply ODP values adapted from Pisso et al. (2010), originally calculated for a VSLS with a lifetime of 20 days, which is very similar to that of $CHBr_3$. ODPs for VSLSs are calculated by means of combining two sources of information: one corresponding to the slow stratospheric branch and the other to the fast tropospheric branch of transport. The former is uniform for all species modelled and is based on the calculation of the expected stratospheric residence time of a Lagrangian particle entering the stratosphere. The latter is based on the probability of stratospheric injection of a given unit emission of the tracer at the ground. The probability of injection depends not only on the fraction of air reaching the tropopause but also on the time the air mass takes from the ground to the tropopause. This is because during the transit of the air mass through the troposphere, the precursor is chemically degraded, and the solubility of the products leads to mass loss due to wet deposition.

In this study, we present the ODP-weighted emissions, which combine the information of the ODP and surface emissions and are calculated by multiplying the $CHBr_3$ emissions with the trajectory-derived ODP at each grid point. The ODP-weighted emissions provide insight into key factors of $CHBr_3$ emission (i.e., where and when $CHBr_3$ is emitted) that impact stratospheric ozone (Tegtmeier et al., 2015). The absolute values are subject to relatively large uncertainties arising from uncertainties in the parameterization of the convective transport. Furthermore, the ODP values applied here do not consider product gas entrainment and provide therefore a lower limit of the impact of $CHBr_3$ on stratospheric ozone. Taking into account product gas entrainment can lead to 30% higher ODP values (Engel and Rigby et al., 2018; Tegtmeier et al., 2020), but has no large impact on the comparison between global ODP-weighted $CHBr_3$ emissions and farm-based ODP-weighted $CHBr_3$ emissions presented here.

## 3. CHBr₃ Emission and Atmospheric Mixing Ratio

### 3.1 CHBr₃ Emissions

As shown in Eq. (2), the total $CHBr_3$ emissions are determined by the growth rate, growth period and initial biomass. For our scenarios based on selected fixed growth rates, the growth periods are adjusted so that the intended annual yield ($\sim 3.5 \times 10^4$ Mg DW) is achieved. We conduct a sensitivity

study to analyze how much the total emissions change for variations of the length and number of the growth periods for a fixed annual yield. For this purpose, we compare Geraldton farming for GTY_O60 (open ocean, six 60 day growth periods) with Geraldton farming for GTY_O96 (open ocean, one 96 day growth period) and Yamba farming for GTY_O60 (terrestrial systems, 73 growth periods of 5 days). Our estimates show that the annual release of $CHBr_3$ from Asparagopsis is the same for all three case studies (Fig. 3a), confirming that for a fixed annual yield and growth rate, the culture conditions of open ocean and tank farming are not important for VSLSs emissions. A second sensitivity study investigates the variations of $CHBr_3$ emissions for different growth rates and the same fixed annual yield. For this purpose, we compare Geraldton farming (open ocean, with an intended annual yield of $\sim1.1\times10^4$ Mg DW) for different growth rates varying between 1% and 10%. The scenario with a 5% growth rate corresponds to Geraldton farming for GTY_O60 (open ocean, six 60 day growth periods), while for the other growth rates the growth periods have been adjusted to achieve the same annual yield.

The $CHBr_3$ emissions depend strongly on the growth rates (Fig 3b), with emission calculated for a 1% growth rate being almost 10 times higher than the emissions calculated for a 10% growth rate. For a lower growth rate, the initial biomass needs to be higher to achieve the targeted seaweed yield ($\sim1.1\times10^4$ Mg) after one year and/or the growth period needs to be longer, thus resulting in larger amounts of biomass in the ocean and higher annual $CHBr_3$ emissions. Vice versa, for higher growth rates, the annual oceanic biomass is smaller and total emissions are lower.

The overall emissions from the intended Australian seaweed farming of $\sim3.5\times10^4$ Mg DW range from 13.5 Mg (0.05 Mmol) for a 10% growth rate to 134 Mg (0.5 Mmol) per year for a 1% growth rate. For the growth rates higher than 5%, the differences of $CHBr_3$ emissions are less significant than those derived for the lower growth rates. In our study, we choose 5% growth rate as representative, which leads to emissions of $\sim27$ Mg (0.1 Mmol) $CHBr_3$ per year for the targeted final yield. For the global scenario with an annual yield of $\sim1.0\times10^6$ Mg DW (30 times of the Australian target), the emissions would range from 412 Mg (1.6 Mmol) to 4014 Mg (16 Mmol) per year, with the annual emission of 810 Mg (3.2 Mmol) for 5% growth rates.

Interestingly, the potential local emissions for all the farming scenarios are generally 3 to 6 orders of magnitude higher than the background coastal emissions. The maximum climatological emissions derived from available observations (Ziska_Coast) are around 2000 pmol m$^{-2}$ hr$^{-1}$ for the coastal waters of Australia, while the emissions from an *Asparagopsis* farm can reach more

than $2.0 \times 10^6$ pmol (2 µmol) m$^{-2}$ hr$^{-1}$ from a terrestrial system and more than $5.0 \times 10^5$ pmol m$^{-2}$ hr$^{-1}$ from the open ocean. These differences are to a large degree related to the fact that the Ziska_Coast is given on a 1.0°x1.0° grid, with high coastal values averaging out over the relatively wide grid cells, while the values derived for the farms apply to much smaller areas. Tank emission rates (0.01°x0.01°) and open ocean farming emission rates (0.1°x0.1°) averaged over a 1°x1° grid cell result in 200 pmol CHBr$_3$ m$^{-2}$ hr$^{-1}$ and 5000 pmol CHBr$_3$ m$^{-2}$ hr$^{-1}$, respectively, thus being very similar to the Ziska emissions.
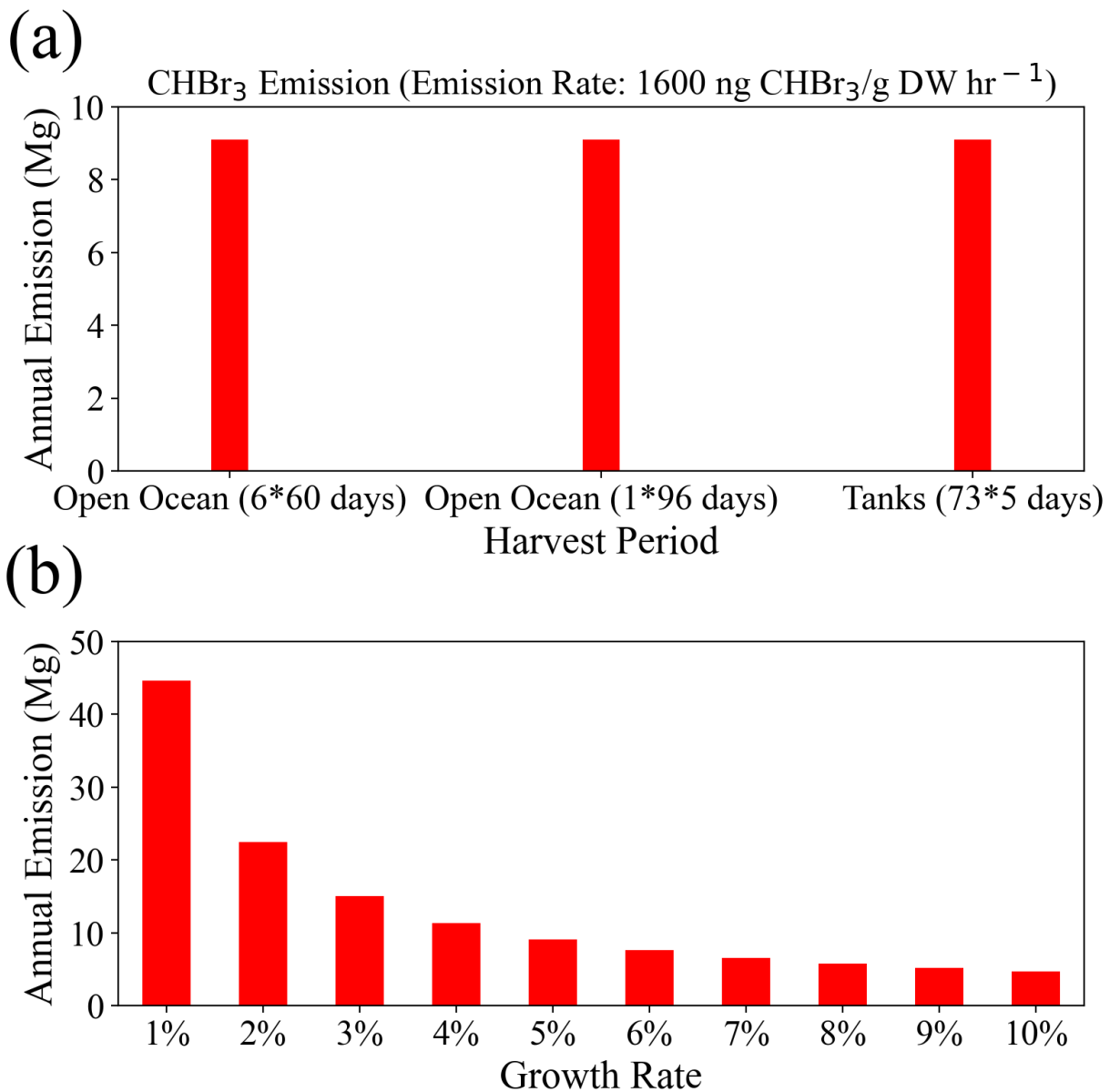
**Figure 3.** The annual release of $CHBr_3$ (Mg yr$^{-1}$) from: a) same growth rate (5%) for different growth periods; and b) under different growth rates but with same initial biomass, both a) and b) are obtained with a total annual yield of 11558 Mg DW.

### 3.2 Atmospheric CHBr$_3$ mixing ratio

We use the $CHBr_3$ emissions calculated in section 3.1 to simulate the enhanced atmospheric $CHBr_3$ mixing ratios (above natural background) for each *Asparagopsis* farming scenario. Background $CHBr_3$ levels are calculated based on the Ziska et al. (2013) Australian coastal emissions (Ziska_Coast). The temporal evolution of $CHBr_3$ mixing ratio with height shows that the $CHBr_3$ resulting from the Australian farming scenarios are negligible (see Figure S1) compared to the coastal background emissions of Australia (Ziska_Coast).

For the global scenarios (Figure 4), atmospheric $CHBr_3$ is comparable to $CHBr_3$ resulting from Australian coastal background emissions, especially near the end of the growth period in the open ocean. For almost all scenarios (except for GTY_O96 _Jul_30x), the emissions generally reach higher into the atmosphere in the first three months of the year with enhanced values around 15 km, reflecting the stronger convection during austral summer. For open ocean emissions occurring during late austral winter (GTY_O96_Jul_30x, Figure 4c), high $CHBr_3$ mixing ratios are found around September, however at a lower altitude range compared to the equivalent scenario with open ocean emission occurring during late austral summer (GTY_O96_Jan_30x; Figure 3b).

The spatial distribution of annual mean $CHBr_3$ at 1 km (Figure 5) further confirms the insignificance of the signals from the Australian farming scenarios compared with the background $CHBr_3$ values. For the global scenarios, localized regions of high mixing ratios are found near the locations of the farms due to the stronger emission. For Darwin_O60_30x, the belt of high mixing ratios is extending northwestward, due to the prevailing easterlies in the tropics. At higher altitudes (e.g., 5 km and 15 km; Figure S2-S3), localized high $CHBr_3$ is only found near Darwin for the Darwin_O60 _30x scenario, reflecting that strong tropical convection is needed to transport short lived gases to such altitudes.

The results above suggest that in the boundary layer, global scenarios and extreme events could lead to $CHBr_3$ comparable mixing ratios as those from the background scenario. Only in the global tropical scenario (Darwin_O60 _30x), $CHBr_3$ mixing ratios, which are larger than the background values, can be found at high altitudes (Figure 4).

427 Simulations of the two extreme scenarios (Geraldton_Ex) for 60 and 96 day growth periods are
428 shown in Figure 6. For the Geraldton_Ex simulations, we assume the implausible scenario that the
429 farm could be totally damaged by cyclone Joyce on the day of harvest in January and the total
430 CHBr$_3$ content of the *Asparagopsis* stock was simultaneously released to the atmosphere during
431 the event. Both scenarios lead to significant CHBr$_3$ mixing ratios in the atmosphere, especially at
432 altitudes below 5 km. Among the two scenarios, the Geraldton_Ex96 contributes the larger amount
433 of CHBr$_3$ emission, as the macroalgae experienced a longer growth period, so the biomass was
434 higher and had accumulated more CHBr$_3$. When averaged over the same period (Jan 9-Jan 26,
435 2018), the CHBr$_3$ mixing ratios from Geraldton_Ex96 are much larger than those from
436 Ziska_Coast (Figure 6) below 5 km, and signals with comparable magnitudes, though with smaller
437 coverage, are found at 15 km.
438 As mentioned in section 3.1, the local CHBr$_3$ emissions due to the seaweed cultivation are
439 generally higher than coastal emission given on 1.0x1.0 grid. However, due to the relatively small
440 spatial extent of the farms, the emissions quickly dilute in the atmosphere, and the magnitude of
441 the mixing ratios decline rapidly off the coast and vertically.
442
443

444
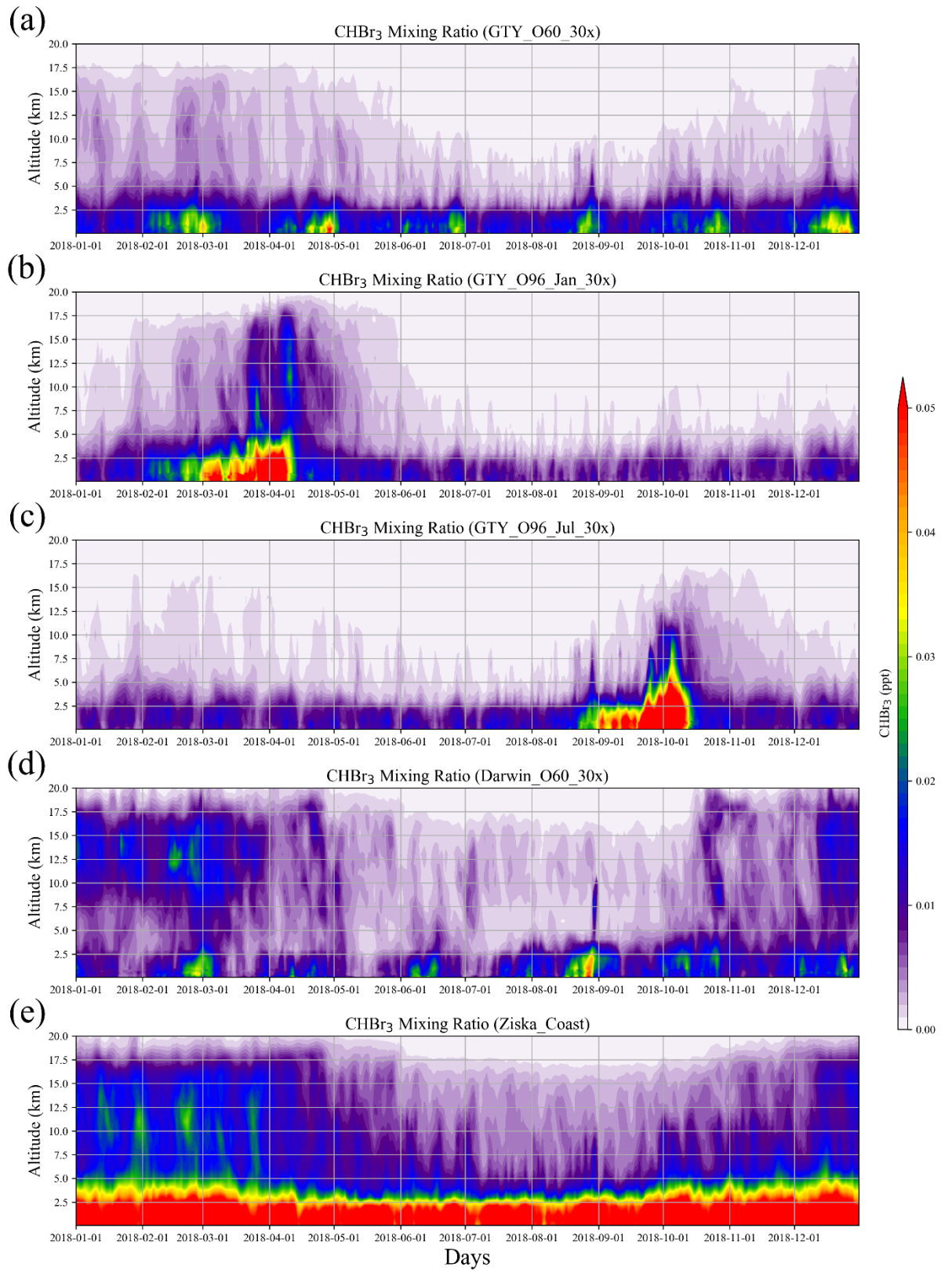
445 **Figure 4.** Altitude-time cross-sections of CHBr$_3$ mixing ratio averaged over [10°-45° S, 105°-
446 165° E] from Global Scenarios: a) GTY_O60_30x, b) GTY_O96_Jan_30x, c)
447 GTY_O96_Jul_30x, d) Darwin_O60 _30x, and Background Scenario: e) Ziska_Coast.
448
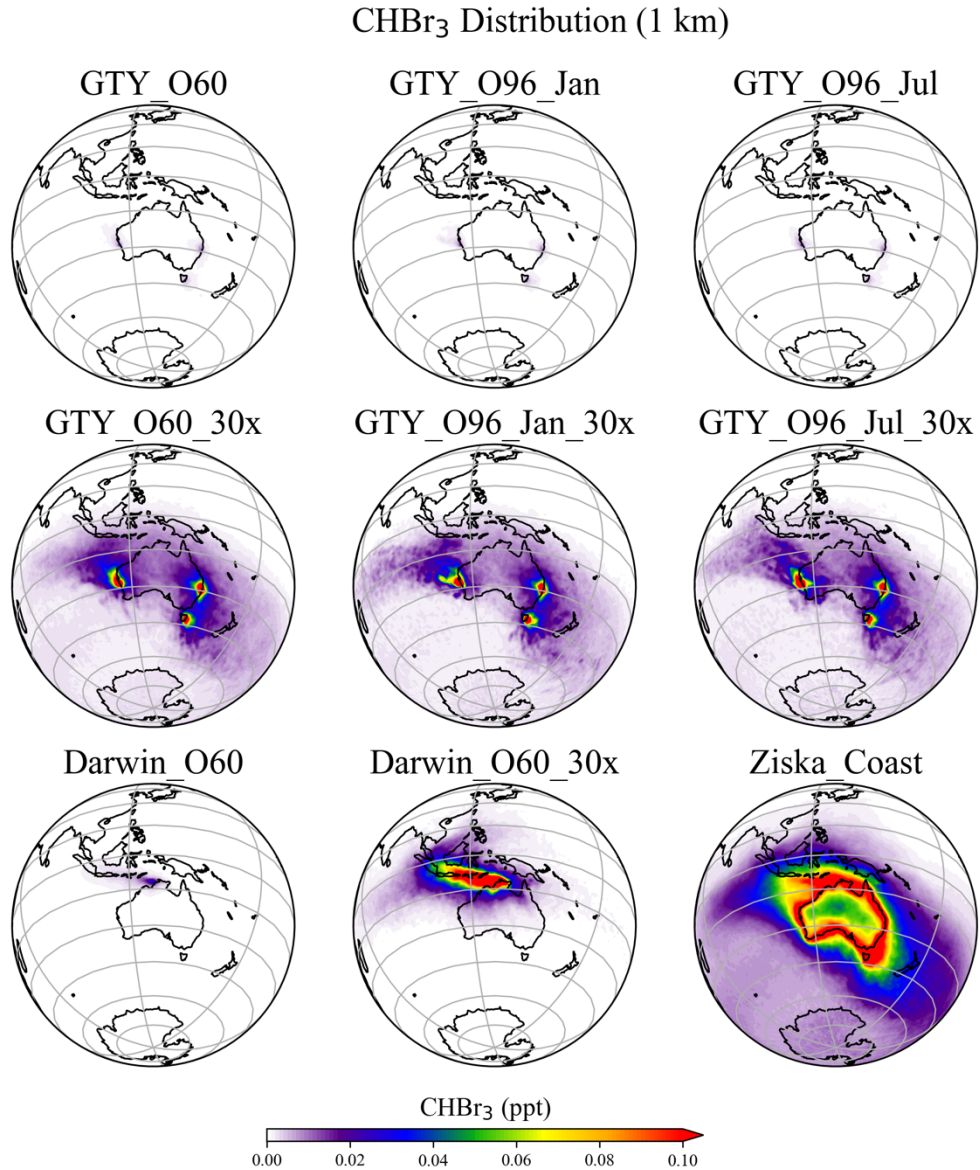
449
450 **Figure 5.** Annual mean CHBr$_3$ spatial distribution from GTY_O60, GTY_O60_30x,
451 GTY_O96_Jan, GTY_O96_Jan_30x, GTY_O96_Jul, GTY_O96_Jul_30x, Darwin_O60,
452 Darwin_O60_30x, and Ziska_Coast at 1 km altitude.
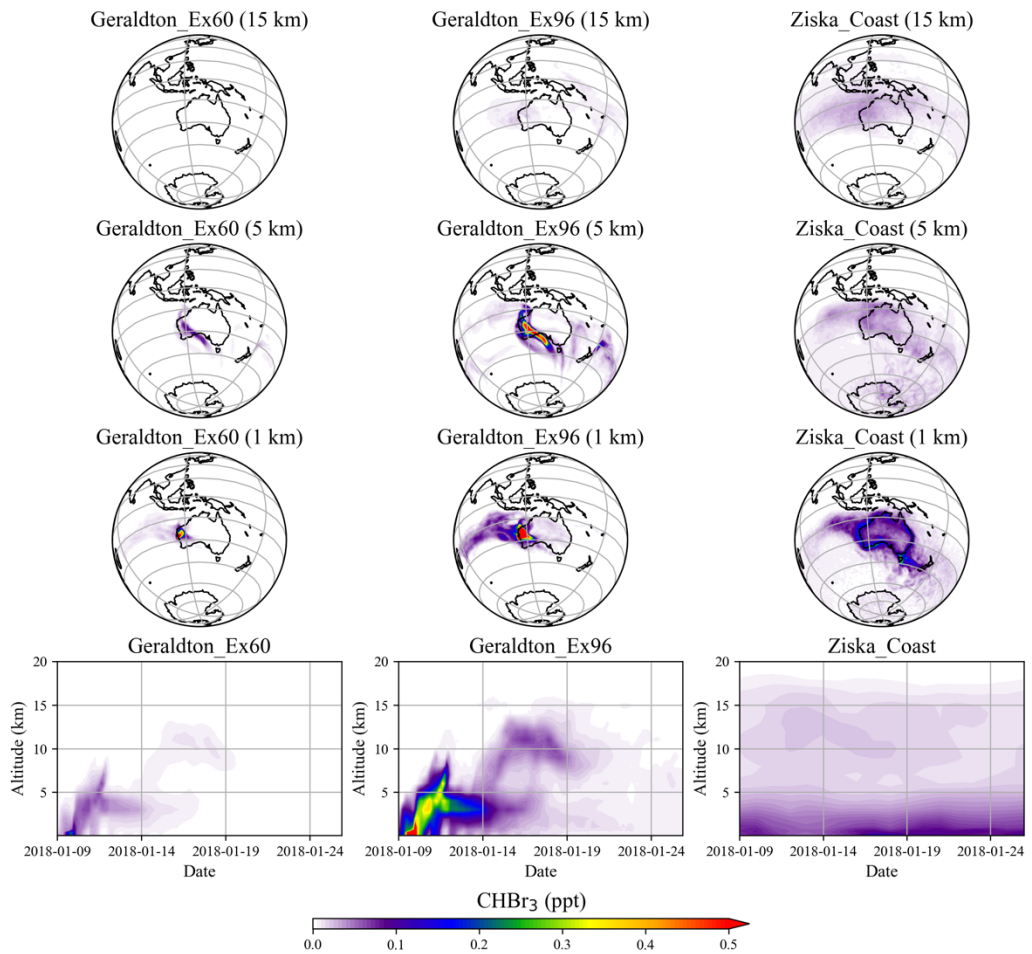
**Figure 6.** 17-day average of spatial distribution and altitude-time cross-sections of $CHBr_3$ mixing ratio averaged over [10°-45° S, 105°-165° E] for Geraldton_Ex60, Geraldton_Ex96, and Ziska_Coast.

## 4. Ozone depletion potential for $CHBr_3$

The ODP distribution from Pisso et al. (2010) for the region around Australia, South-East Asia, and the Indian Ocean for the Southern Hemisphere (SH) summer and winter is shown in Figure 7. The ODP distribution changes strongly with season as the transport of short-lived halogenated substances such as $CHBr_3$ depends on the seasonal variations of the location of the Intertropical Convergence Zone (ITCZ). Highest ODP values of 0.5, which imply that any amount (per mass) of $CHBr_3$ released from the specific location will destroy half as much stratospheric ozone as the same amount of CFC-11 released from this location, are found during July over the Maritime continent and during January over the West Pacific south of the equator. The northern Australian

coastline shows highest ODP values during January when the thermal equator and the ITCZ are shifted southwards and ODP values for Yamba and Darwin are 0.26 and 0.29, respectively. The other two locations as well as all four locations during SH winter, show ODP values of only up to 0.1.

As demonstrated in section 3, the total annual $CHBr_3$ emissions from any location are independent of the details of the farming practice, however, the ODP-weighted emissions change for the different scenarios as the growth periods fall into different seasons with varying ODP values. In general, the scenario of one harvest period in SH summer leads to larger ODP-weighted emissions when compared to the same biomass harvested throughout the year. In addition to the harvesting practice, the locations of the farms have a large impact on the efficiency of the $CHBr_3$ transport to the stratosphere and thus on the ODP-weighted emissions.

The ODP-weighted emissions of $CHBr_3$ for different emission scenarios are shown in Figure 8. *Asparagopsis* farming at GTY (GTY_O60) leads to additional $CHBr_3$ emissions of up to 2.53 Mg per year. If all farming ($\sim3.5\times10^4$ Mg DW *Asparagopsis*) occurs in Darwin (Darwin_O60), ODP-weighted emissions would increase to 6.48 Mg $CHBr_3$ per year. In comparison, all naturally occurring emissions around the Australian coastline (Ziska_coast) lead to OPD-weighted $CHBr_3$ emissions of 221.52 Mg per year. In consequence, *Asparagopsis* farming in the three locations Geraldton, Triabunna and Yamba would lead to an increase of the ODP-weighted emissions from Australian coastal emissions of 1.14%. If all farming would take place in Darwin, ODP-weighted $CHBr_3$ emissions would increase by 2.93%.

As the global ODP-weighted emissions were estimated to be around $4.0\times10^4$ Mg per year (bottom-most bar in Figure 8., Tegtmeier et al., 2015), the additional contribution due to the Australian farming scenarios in GTY or Darwin would be negligible increasing the contribution of $CHBr_3$ emissions to ozone depletion by 0.006% and 0.016%, respectively. Even if the farming would be upscaled to cover the global needs ($\sim1.0\times10^6$ Mg DW), the ODP-weighted $CHBr_3$ emissions would only increase to 75 Mg and 195 Mg for farming in GTY (GTY_O60_30x) and Darwin (Darwin_O60_30x), respectively. Thus produced $CHBr_3$ would increase the current contribution of $CHBr_3$ to stratospheric ozone depletion by 0.19% and 0.48%, which is again a very small contribution.

To assess the increase of the ODP-weighted $CHBr_3$ emissions under the most extreme and implausible conditions, we envision the total harvest of one year, which contains 752 Mg (21.7

500   mg CHBr$_3$/g DW*34674 Mg DW) CHBr$_3$, stored in a warehouse of 50 x 25 x 5 m in either of the

501   four locations.  We assume that the facility is destroyed, and all 750 Mg released to the atmosphere.

502   Then maximum ODP-weighted CHBr$_3$ emissions would occur for the release in Darwin during

503   January and amount to 215.9 Mg almost doubling the ODP-weighted coastal CHBr$_3$ emissions of

504   Australia. If the entire content of ~$1.0\times10^6$ Mg *Asparagopsis* DW (21.7 mg CHBr$_3$/g DW*1040220

505   Mg DW=22573 Mg CHBr$_3$) would be released in Darwin, the additional contribution of CHBr$_3$ to

506   global ozone depletion could reach 16%.

507
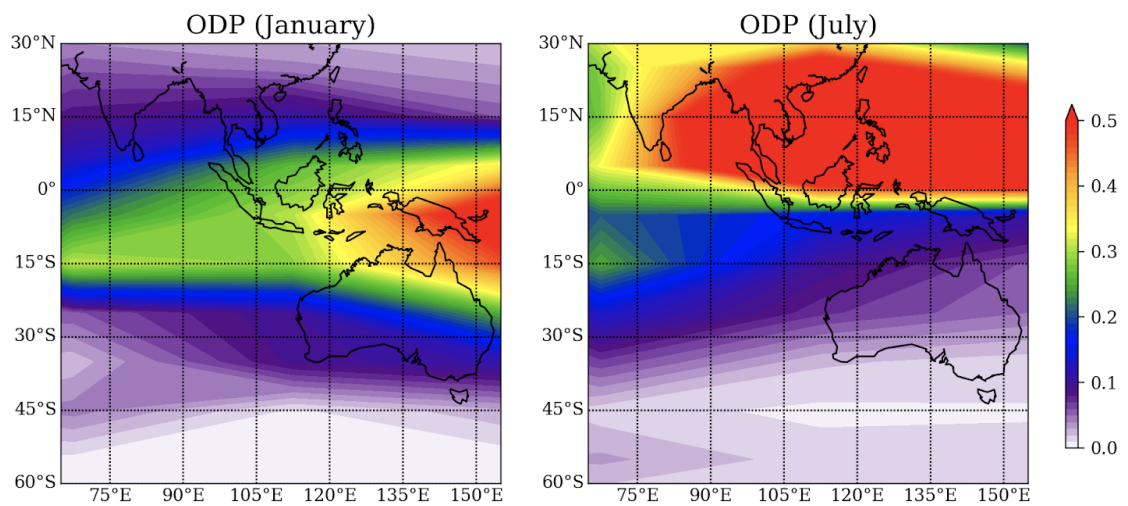
508
509   **Figure 7.** Spatial distribution of the ODP in January and July from Pisso et al. (2010), plotted with
510   interval of 0.01.
511
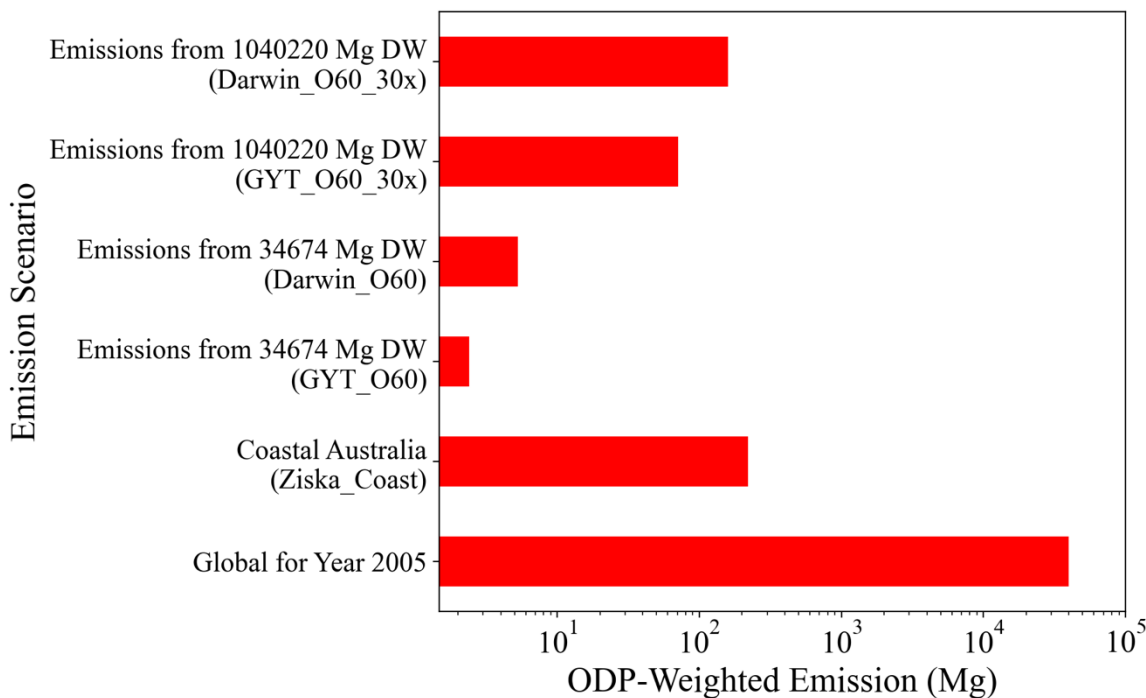
**Figure 8.** The ODP-weighted emissions of $CHBr_3$ for Global Scenarios (GTY_O60_30x and Darwin_O60_30x), Australian Scenarios (GTY_O60 and Darwin_O60), Coastal Australian emission (Ziska_Coast), and global ODP-weighted emission for 2005 taken from Tegtmeier et al. (2015) as a reference, note that the x-axis is exponential.

## 5. Summary and Conclusions

In this study, we assessed the potential risks of $CHBr_3$ released from *Asparagopsis* farming near Australia for the stratospheric ozone layer by analyzing different cultivation scenarios. We conclude that the intended operation of *Asparagopsis* seaweed cultivation farms with an annual yield of 34674 Mg DW in either open ocean or terrestrial cultures at the locations Triubanna, Yamba, Geraldton, and Darwin will not impact the ozone layer under normal operating conditions. For Australia scenarios with an annual yield of $\sim 3.5 \times 10^4$ Mg DW and algae growth rate of 5% per day, the expected annual $CHBr_3$ emission from the considered *Asparagopsis* farms into the atmosphere ($\sim$27 Mg, 0.11 Mmol) is less than 0.9% of the coastal Australian emissions ($\sim$3109 Mg, 12.3 Mmol). This contribution is negligible from a global perspective by adding less than 0.01% to the worldwide $CHBr_3$ emissions from natural and anthropogenic sources. The overall emissions from the farms would be even smaller with a faster growth rate for the same annual

yield. We have assumed a high $CHBr_3$ production of 21.7 mg/g DW from superior strains and expected lower $CHBr_3$ production of 14 mg/g DW would likewise reduce emissions to the atmosphere.

The $CHBr_3$ emissions from the localized *Asparagopsis* farms could be larger than emissions from coastal Australia. However, the overall atmospheric impact of the *Asparagopsis* farms is negligible, as the $CHBr_3$ dilutes rapidly and degrades in the atmosphere under normal weather conditions. Mixing ratios of $CHBr_3$ are generally dominated by the coastal Australian emissions. In global scenarios with annual yield ~1.0 $\times 10^6$ Mg DW, localized $CHBr_3$ mixing ratios comparable to the background values can be found in the lower troposphere. In the upper troposphere, on the other hand, mixing ratios larger than background values only appear in the global tropical scenario (Darwin_O60 _30x). The release of the complete $CHBr_3$ content from the macroalgae to the environment on very short timescales (e.g., days) due to extreme weather situations could contribute significant amounts to the atmosphere, especially during times when the standing stock biomass is relatively large (Geraldton_Ex96). While such extreme scenarios could lead to much larger mixing ratios than background values, such mass release events are implausible because even if a farm was totally destroyed the seaweed stock could not instantaneously release all the accumulated $CHBr_3$. Such scenarios have been included here to evaluate a catastrophic and likely impossible worst-case scenario.

The impact of $CHBr_3$ from the proposed seaweed farms on the stratospheric ozone layer is assessed by weighting the emissions with the ozone depletion potential of $CHBr_3$. In total, Australia scenarios could lead to additional ODP-weighted $CHBr_3$ emissions of up to 2.53 Mg per year with farms located in Geraldton, Triubana and Yamba. With all farming performed in Darwin (Darwin_O60), the emitted $CHBr_3$ could reach the stratosphere on shorter time scales and ODP-weighted emissions would increase to 6.48 Mg, which is less than 0.02% of the global ODP-weighted emissions. For global tropical scenario (Darwin_O60_30x), the ODP-weighted emissions amount to 175 Mg, increasing the global ozone depletion by 0.48%, resulting in a very small contribution. The ODP used in this study, does not include the impact of VSLS product gases. Previous modelling studies have highlighted the role of product gas treatment and their impact on the stratospheric halogen budget (e.g., Fernandez et al., 2021). Including product gas entrainment can lead to up to 30% larger ODP values for $CHBr_3$ (Engel and Rigby et al., 2018; Tegtmeier et al., 2020), thus the ODP-weighted emissions presented here can be up to 30% larger.

564 However, this does not affect our assessment of the potential importance of cultivation induced
565 $CHBr_3$ as the ratios of the impact of each scenario compared with the global ODP-weighted
566 emission remain the same. Another point to note is that Ziska emission potentially underestimate
567 background levels of $CHBr_3$ in coastal regions (Ziska et al., 2013), e.g. $CHBr_3$ measurement in
568 Cape Grim, which is close to Triabunna, shows much larger $CHBr_3$ mixing ratio (~1.5 ppt, Dunse
569 et al., 2020). However, including such higher atmospheric background values in the Ziska
570 methodology would not really increase the fluxes as the flux is driven by air-sea gradient (Eq. 3).
571 Our conclusions will still hold if stronger coastal emission is applied, as it will increase the
572 background $CHBr_3$ mixing ratios.
573 We note that all data characterizing the potential systems for the production of *Asparagopsis* are
574 based on few available literature data, laboratory scale tests and relatively small-scale field trials.
575 This not only places limitations on the technological representativeness of a future system and the
576 temporal validity of the study, but also demonstrates importance for directed studies, especially on
577 the release of $CHBr_3$ from *Asparagopsis* during cultivation. As this understanding evolves so will
578 the cultivation and processing technologies engineered to conserve the antimethanogenic $CHBr_3$
579 in the seaweed biomass which is the primary value feature of *Asparagopsis*. These limitations are
580 largely mitigated in our study by evaluating various environmental and meteorological conditions
581 ranging from conservative to most extreme scenarios and by investigating different farming
582 practices based on various sensitivity studies.
583

584 **Data availability**
585 The $CHBr_3$ emission data and FLEXPART output can be obtained from the authors on request via
586 BQ (bquack@geomar.de), ST (susann.tegtmeier@usask.ca), or YJ (yue.jia@noaa.gov).
587

588 **Author Contributions**
589 BQ initialized the idea. YJ, BQ, and ST carried out the calculations and analysis. YJ performed
590 the FLEXPART simulations and produced the figures. YJ, BQ, and ST wrote the manuscript with
591 the contribution from other co-authors RK and IP. RK contributed to conceptualization, design,
592 writing, editing, procurement of funding. All the authors contributed to discussions and revisions
593 of the manuscript.
594

595 **Competing interests**

596 The authors declare that they have no conflict of interest.

597
598 **Acknowledgements**

599 The authors wish to acknowledge CSIRO, FutureFeed, and Sea Forest for their provision of
600 technical knowledge, data, and insight into Asparagopsis supply chains in Australia. The authors
601 would like to thank the European Centre for Medium-Range Weather Forecasts (ECMWF) for the
602 ERA-Interim reanalysis data and the FLEXPART development team for the Lagrangian particle
603 dispersion model used in this publication. The FLEXPART simulations were performed on
604 resources provided by the University of Saskatchewan.

**Reference**

Abbott, D. W., Aasen, I. M., Beauchemin, K. A., Grondahl, F., Gruninger, R., Hayes, M., Huws, S., Kenny, D. A., Krizsan, S. J., Kirwan, S. F., Lind, V., Meyer, U., Ramin, M., Theodoridou, K., von Soosten, D., Walsh, P. J., Waters, S., and Xing, X.: Seaweed and Seaweed Bioactives for Mitigation of Enteric Methane: Challenges and Opportunities, Animals, 10, 2432, https://doi.org/10.3390/ani10122432, 2020.

Aschmann, J., Sinnhuber, B. M., Atlas, E. L., and Schauffler, S. M.: Modeling the transport of very short-lived substances into the tropical upper troposphere and lower stratosphere, Atmos. Chem. Phys., 9, 9237-9247, 10.5194/acp-9-9237-2009, 2009.

Battaglia, M. CSIRO and FutureFeed Pty Ltd. Personal Communication. 2020. https://www.csiro.au/ and https://www.future-feed.com/

Beauchemin, K. A., Ungerfeld, E. M., Eckard, R. J., and Wang, M.: Review: Fifty years of research on rumen methanogenesis: lessons learned and future challenges for mitigation, Animals, 14, S2-S16, https://doi.org/10.1017/S1751731119003100, 2020.

Black, J. L., Davison, T. M., Box, I.: Methane Emissions from Ruminants in Australia: Mitigation Potential and Applicability of Mitigation Strategies. Animals, 11, 951. https://doi.org/10.3390/ani11040951, 2021

Brioude, J., Portmann, R. W., Daniel, J. S., Cooper, O. R., Frost, G. J., Rosenlof, K. H., Granier, C., Ravishankara, A. R., Montzka, S. A., and Stohl, A.: Variations in ozone depletion potentials of very short-lived substances with season and emission region, Geophysical Research Letters, 37, https://doi.org/10.1029/2010GL044856, 2010.

Burreson, B. J., Moore, R. E., and Roller, P. P.: Volatile halogen compounds in the alga Asparagopsis taxiformis (Rhodophyta), Journal of Agricultural and Food Chemistry, 24, 856-861, 10.1021/jf60206a040, 1976.

Carpenter, L. J., and Liss, P. S.: On temperate sources of bromoform and other reactive organic bromine gases, Journal of Geophysical Research: Atmospheres, 105, 20539-20547, https://doi.org/10.1029/2000JD900242, 2000.

Carpenter, L. J., Reimann, S. (Lead Authors), Burkholder, J. B., Clerbaux, C., Hall, B. D., and Hossaini, R.: Ozone-depleting substances (ODSs) and other gases of interest to the Montreal Protocol. In: Scientific assessment of ozone depletion: 2014. Global Ozone Research and Monitoring Project-Report A., E. and A., M. S. (Eds.), World Meteorological Organization., Geneva, Switzerland, 2014.

Claxton, T., R. Hossaini, O. Wild, M.P. Chipperfield, and C. Wilson, On the regional and seasonal ozone depletion potential of chlorinated very shortlived substances, Geophys. Res. Lett., 46(10), 5489–5498. doi:10.1029/2018GL081455, 2019.

Dee, D. P., Uppala, S. M., Simmons, A. J., Berrisford, P., Poli, P., Kobayashi, S., Andrae, U., Balmaseda, M. A., Balsamo, G., Bauer, P., Bechtold, P., Beljaars, A. C. M., van de Berg, L., Bidlot, J., Bormann, N., Delsol, C., Dragani, R., Fuentes, M., Geer, A. J., Haimberger, L., Healy, S. B., Hersbach, H., Holm, E. V., Isaksen, L., Kallberg, P., Kohler, M., Matricardi, M., McNally, A. P., Monge-Sanz, B. M., Morcrette, J. J., Park, B. K., Peubey, C., de Rosnay, P., Tavolato, C., Thepaut, J. N., and Vitart, F.: The ERA-Interim reanalysis: configuration and performance of the data assimilation system, Q J Roy Meteor Soc, 137, 553-597, https://doi.org/10.1002/qj.828, 2011.

Dunse, B. L., Derek, N., Fraser, P. J., Krummel, P. B., and Steele, L. P.: Australian and Global Emissions of Ozone Depleting Substances, Report prepared for the Australian Government Department of Agriculture, Water and the Environment, CSIRO Oceans and Atmosphere, Climate Science Centre, Melbourne, Australia, viii, 58 p., 2020.

Elsom, S. Sea Forest Asparagopsis production. Personal Communication. https://www.seaforest.com.au/, 2020.

Engel, A., and Rigby, M. (Lead Authors), Burkholder, J. B., Fernandez, R. P., Froidevaux, L., Hall, B. D., Hossaini, R., Saito, T., Vollmer, M. K., and Yao, B.: Update on Ozone-Depleting Substances (ODSs) and Other Gases of Interest to the Montreal Protocol, Chapter 1 in Scientific Assessment of Ozone Depletion: 2018, Global Ozone Research and Monitoring Project — Report No. 58, World Meteorological Organization, Geneva, Switzerland, 2018.

Fernandez, R. P., Barrera, J. A., López-Noreña, A. I., Kinnison, D. E., Nicely, J., Salawitch, R. J., Wales, P. A., Toselli, B. M., Tilmes, S., Lamarque, J.-F., Cuevas, C. A., and Saiz-Lopez, A.: Intercomparison between surrogate, explicit and full treatments of VSL bromine chemistry within the CAM-Chem chemistry-climate model. Geophysical Research Letters, 48, e2020GL091125. https://doi.org/10.1029/2020GL091125, 2021.

Forster, C., Stohl, A., and Seibert, P.: Parameterization of Convective Transport in a Lagrangian Particle Dispersion Model and Its Evaluation, Journal of Applied Meteorology and Climatology, 46, 403-422, 10.1175/jam2470.1, 2007.

Gerber, P.J., Steinfeld, H., Henderson, B., Mottet, A., Opio, C., Dijkman, J., Falcucci, A. & Tempio, G.: Tackling climate change through livestock – A global assessment of emissions and mitigation opportunities. Food and Agriculture Organization of the United Nations (FAO), Rome, 2013.

Hense, I., and Quack, B.: Modelling the vertical distribution of bromoform in the upper water column of the tropical Atlantic Ocean, Biogeosciences, 6, 535-544, 10.5194/bg-6-535-2009, 2009.

Herrero, M., and Thornton, P. K.: Livestock and global change: Emerging issues for sustainable food systems, Proceedings of the National Academy of Sciences, 110, 20878-20881, 10.1073/pnas.1321844111, 2013.

695 Hossaini, R., Chipperfield, M. P., Monge-Sanz, B. M., Richards, N. A. D., Atlas, E., and Blake,
696 D. R.: Bromoform and dibromomethane in the tropics: a 3-D model study of chemistry and
697 transport, Atmos. Chem. Phys., 10, 719-735, 10.5194/acp-10-719-2010, 2010.
698
699 Hung, L. D., Hori, K., Nang, H. Q., Kha, T., and Hoa, L. T.: Seasonal changes in growth rate,
700 carrageenan yield and lectin content in the red alga Kappaphycus alvarezii cultivated in Camranh
701 Bay, Vietnam, Journal of Applied Phycology, 21, 265-272, 10.1007/s10811-008-9360-2, 2009.
702
703 IPCC: Climate Change 2022: The Physical Science Basis. Contribution of Working Groups I to
704 the Sixth Assessment Report of the Intergovernmental Panel on Climate Change IPCC, Geneva,
705 Switzerland, 2021.
706
707 Kamra, D. N.: Rumen microbial ecosystem, Curr Sci India, 89, 124-135,
708 http://www.jstor.org/stable/24110438, 2005.
709
710 Kinley, R. D. and Fredeen, A. H.: In Vitro Evaluation of Feeding North Atlantic Stormtoss
711 Seaweeds on Ruminal Digestion. Journal of Applied Phycology, 27, 2387 2393.
712 http://dx.doi.org/10.1007/s10811-014-0487-z, 2015.
713
714 Kinley, R., Vucko, M., Machado, L., and Tomkins, N.: In Vitro Evaluation of the
715 Antimethanogenic Potency and Effects on Fermentation of Individual and Combinations of Marine
716 Macroalgae. American Journal of Plant Sciences, 7, 2038-2054. doi: 10.4236/ajps.2016.714184,
717 2016a.
718
719 Kinley, R. D., de Nys, R., Vucko, M. J., Machado, L., and Tomkins, N. W.: The red
720 macroalgae *Asparagopsis taxiformis* is a potent natural antimethanogenic that reduces methane
721 production during *in vitro* fermentation with rumen fluid, Animal Production Science, 56, 282-289,
722 https://doi.org/10.1071/AN15576, 2016b.
723
724 Kinley, R. D., Martinez-Fernandez, G., Matthews, M. K., de Nys, R., Magnusson, M., and
725 Tomkins, N. W.: Mitigating the carbon footprint and improving productivity of ruminant livestock
726 agriculture using a red seaweed, Journal of Cleaner Production, 259, 120836,
727 https://doi.org/10.1016/j.jclepro.2020.120836, 2020.
728
729 Leedham, E. C., Hughes, C., Keng, F. S. L., Phang, S. M., Malin, G., and Sturges, W. T.: Emission
730 of atmospherically significant halocarbons by naturally occurring and farmed tropical macroalgae,
731 Biogeosciences, 10, 3615-3633, 10.5194/bg-10-3615-2013, 2013.
732
733 Li, X. X., Norman, H. C., Kinley, R. D., Laurence, M., Wilmot, M., Bender, H., de Nys, R., and
734 Tomkins, N.: Asparagopsis taxiformis decreases enteric methane production from sheep, Animal
735 Production Science, 58, 681-688, https://doi.org/10.1071/AN15883, 2018.
736
737 Liang, Q., Stolarski, R. S., Kawa, S. R., Nielsen, J. E., Douglass, A. R., Rodriguez, J. M., Blake,
738 D. R., Atlas, E. L., and Ott, L. E.: Finding the missing stratospheric $Br_y$: a global
739 modeling study of $CHBr_3$ and $CH_2Br_2$, Atmos. Chem.
740 Phys., 10, 2269-2286, 10.5194/acp-10-2269-2010, 2010.
741

742     Maas, J., Tegtmeier, S., Quack, B., Biastoch, A., Durgadoo, J. V., Ruhs, S., Gollasch, S., and
743     David, M.: Simulating the spread of disinfection by-products and anthropogenic bromoform
744     emissions from ballast water discharge in Southeast Asia, Ocean Sci, 15, 891-904, 10.5194/os-15-
745     891-2019, 2019.
746
747     Maas, J., Tegtmeier, S., Jia, Y., Quack, B., Durgadoo, J. V., and Biastoch, A.: Simulations of
748     anthropogenic bromoform indicate high emissions at the coast of East Asia, Atmos. Chem. Phys.,
749     21, 4103-4121, 10.5194/acp-21-4103-2021, 2021.
750
751     Machado, L., Magnusson, M., Paul, N. A., de Nys, R., and Tomkins, N.: Effects of Marine and
752     Freshwater Macroalgae on In Vitro Total Gas and Methane Production, PLOS ONE, 9, e85289,
753     10.1371/journal.pone.0085289, 2014.
754
755     Machado, L., Magnusson, M., Paul, N. A., Kinley, R., de Nys, R., and Tomkins, N. W.:
756     Identification of bioactives from the red seaweed Asparagopsis taxiformis that promote
757     antimethanogenic activity in vitro, J. Appl. Phycol., 28, 3117-3126,
758     https://doi.org/10.1007/s10811-016-0830-7, 2016.
759
760     Magnusson, M., Vucko, M. J., Neoh, T. L., and de Nys, R.: Using oil immersion to deliver a
761     naturally-derived, stable bromoform product from the red seaweed Asparagopsis taxiformis, Algal
762     Research, 51, 102065, https://doi.org/10.1016/j.algal.2020.102065, 2020.
763
764     Marshall, R. A., Harper, D. B., McRoberts, W. C., and Dring, M. J.: Volatile bromocarbons
765     produced by Falkenbergia stages of Asparagopsis spp. (Rhodophyta), Limnology and
766     Oceanography, 44, 1348-1352, doi: 10.4319/lo.1999.44.5.1348, 1999.
767
768     Mata, L., Gaspar, H., and Santos, R.: CARBON/NUTRIENT BALANCE IN RELATION TO
769     BIOMASS PRODUCTION AND HALOGENATED COMPOUND CONTENT IN THE RED
770     ALGA ASPARAGOPSIS TAXIFORMIS (BONNEMAISONIACEAE)1, Journal of Phycology,
771     48, 248-253, https://doi.org/10.1111/j.1529-8817.2011.01083.x, 2012.
772
773     Mata, L., Lawton, R. J., Magnusson, M., Andreakis, N., de Nys, R., and Paul, N. A.: Within-
774     species and temperature-related variation in the growth and natural products of the red alga
775     Asparagopsis taxiformis, Journal of Applied Phycology, 29, 1437-1447, 10.1007/s10811-016-
776     1017-y, 2017.
777
778     Mayberry, D., Bartlett, H., Moss, J., Davison, T., and Herrero, M.: Pathways to carbon-neutrality
779     for the Australian red meat sector, Agricultural Systems, 175, 13-21,
780     https://doi.org/10.1016/j.agsy.2019.05.009, 2019.
781
782     Moate, P. J., Deighton, M. H., Williams, S. R. O., Pryce, J. E., Hayes, B. J., Jacobs, J. L., Eckard,
783     R. J., Hannah, M. C., and Wales, W. J.: Reducing the carbon footprint of Australian milk
784     production by mitigation of enteric methane emissions, Animal Production Science, 56, 1017-
785     1034, https://doi.org/10.1071/AN15222, 2016.
786

787 Moore, R. M., Geen, C. E., and Tait, V. K.: Determination of Henry's Law constants for a suite of
788 naturally occurring halogenated methanes in seawater, Chemosphere, 30, 1183-1191,
789 https://doi.org/10.1016/0045-6535(95)00009-W, 1995a.
790
791 Moore, R. M., Tokarczyk, R., Tait, V. K., Poulin, M., and Geen, C.: Marine phytoplankton as a
792 natural source of volatile organohalogens. In: Naturally-Produced Organohalogens, Grimvall, A.
793 and de Leer, E. W. B. (Eds.), Springer Netherlands, Dordrecht, 1995b.
794
795 Morgavi, D. P., Forano, E., Martin, C., and Newbold, C. J.: Microbial ecosystem and
796 methanogenesis in ruminants, Animal, 4, 1024-1036, 10.1017/s1751731110000546, 2010.
797
798 Montzka, S. A. and Reimann, S. et al.: Ozone-depleting substances andrelated chemicals, in
799 Scientific Assessment of Ozone Depletion:2010, Global Ozone Research and Monitoring Project
800 – ReportNo. 52, WMO, Geneva, Switzerland, 2011.
801
802 Nightingale, P. D., Malin, G., and Liss, P. S.: Production of chloroform and other low molecular-
803 weight halocarbons by some species of macroalgae, Limnology and Oceanography, 40, 680-689,
804 https://doi.org/10.4319/lo.1995.40.4.0680, 1995.
805
806 Nightingale, P. D., Malin, G., Law, C. S., Watson, A. J., Liss, P. S., Liddicoat, M. I., Boutin, J.,
807 and Upstill-Goddard, R. C.: In situ evaluation of air-sea gas exchange parameterizations using
808 novel conservative and volatile tracers, Global Biogeochemical Cycles, 14, 373-387,
809 https://doi.org/10.1029/1999GB900091, 2000.
810
811 Patra, A. K.: Enteric methane mitigation technologies for ruminant livestock: a synthesis of current
812 research and future directions, Environ Monit Assess, 184, 1929-1952, 10.1007/s10661-011-2090-
813 y, 2012.
814
815 Paul, N. A., de Nys, R., and Steinberg, P. D.: Chemical defence against bacteria in the red alga
816 Asparagopsis armata: linking structure with function, Marine Ecology Progress Series, 306, 87-
817 101, 10.3354/meps306087, 2006.
818
819 Pisso, I., Haynes, P. H., and Law, K. S.: Emission location dependent ozone depletion potentials
820 for very short-lived halogenated species, Atmos. Chem. Phys., 10, 12025-12036, 10.5194/acp-10-
821 12025-2010, 2010.
822
823 Pisso, I., Sollum, E., Grythe, H., Kristiansen, N. I., Cassiani, M., Eckhardt, S., Arnold, D., Morton,
824 D., Thompson, R. L., Groot Zwaaftink, C. D., Evangeliou, N., Sodemann, H., Haimberger, L.,
825 Henne, S., Brunner, D., Burkhart, J. F., Fouilloux, A., Brioude, J., Philipp, A., Seibert, P., and
826 Stohl, A.: The Lagrangian particle dispersion model FLEXPART version 10.4, Geosci. Model
827 Dev., 12, 4955-4997, 10.5194/gmd-12-4955-2019, 2019.
828
829 Quack, B., and Wallace, D. W. R.: Air-sea flux of bromoform: Controls, rates, and implications,
830 Global Biogeochemical Cycles, 17, https://doi.org/10.1029/2002GB001890, 2003.
831

832 Roque, B. M., Venegas, M., Kinley, R. D., de Nys, R., Duarte, T. L., Yang, X., and Kebreab, E.:
833 Red seaweed (Asparagopsis taxiformis) supplementation reduces enteric methane by over 80
834 percent in beef steers, PLOS ONE, 16, e0247820, 10.1371/journal.pone.0247820, 2021.
835
836 Sinnhuber, B.-M., and Meul, S.: Simulating the impact of emissions of brominated very short lived
837 substances on past stratospheric ozone trends, Geophysical Research Letters, 42, 2449-2456,
838 https://doi.org/10.1002/2014GL062975, 2015.
839
840 Stohl, A., Hittenberger, M., and Wotawa, G.: Validation of the lagrangian particle dispersion
841 model FLEXPART against large-scale tracer experiment data, Atmospheric Environment, 32,
842 4245-4264, https://doi.org/10.1016/S1352-2310(98)00184-8, 1998.
843
844 Stohl, A. and Thomson, D.: A density correction for Lagrangian particle dispersion models,
845 Boundary-Layer Meteorology, 90, 155-167, 10.1023/A:1001741110696, 1999.
846
847 Stohl, A. and Trickl, T.: A textbook example of long-range transport: Simultaneous observation
848 of ozone maxima of stratospheric and North American origin in the free troposphere over Europe,
849 Journal of Geophysical Research: Atmospheres, 104, 30445-30462, 10.1029/1999JD900803,1999.
850
851 Tegtmeier, S., Ziska, F., Pisso, I., Quack, B., Velders, G. J. M., Yang, X., and Krüger, K.: Oceanic
852 bromoform emissions weighted by their ozone depletion potential, Atmos. Chem. Phys., 15,
853 13647-13663, 10.5194/acp-15-13647-2015, 2015.
854
855 Tegtmeier, S., Atlas, E., Quack, B., Ziska, F., and Krüger, K.: Variability and past long-term
856 changes of brominated very short-lived substances at the tropical tropopause, Atmos. Chem. Phys.,
857 20, 7103-7123, 10.5194/acp-20-7103-2020, 2020.
858
859 Vucko, M. J., Magnusson, M., Kinley, R. D., Villart, C., and de Nys, R.: The effects of processing
860 on the in vitro antimethanogenic capacity and concentration of secondary metabolites of
861 Asparagopsis taxiformis, J. Appl. Phycol., 29, 1577-1586, 10.1007/s10811-016-1004-3, 2017.
862
863 Wuebbles, D. J.: Chlorocarbon Emission Scenarios - Potential Impact on Stratospheric Ozone,
864 Journal of Geophysical Research-Oceans, 88, 1433-1443, 10.1029/JC088iC02p01433, 1983.
865
866 Yang, X., Abraham, N. L., Archibald, A. T., Braesicke, P., Keeble, J., Telford, P. J., Warwick, N.
867 J., and Pyle, J. A.: How sensitive is the recovery of stratospheric ozone to changes in
868 concentrations of very short-lived bromocarbons?, Atmospheric Chemistry and Physics, 14,
869 10431-10438, 10.5194/acp-14-10431-2014, 2014.
870
871 Yong, Y. S., Yong, W. T. L., and Anton, A.: Analysis of formulae for determination of seaweed
872 growth rate, Journal of Applied Phycology, 25, 1831-1834, 10.1007/s10811-013-0022-7, 2013.
873
874 Zhang, J., Wuebbles, D. J., Kinnison, D. E., and Saiz-Lopez, A.: Revising the ozone depletion
875 potentials metric for short-lived chemicals such as CF3I and CH3I, J. Geophys. Res. Atmos., 125,
876 e2020JD032414, https://doi.org/10.1029/2020JD032414, 2020.
877

878    Ziska, F., Quack, B., Abrahamsson, K., Archer, S. D., Atlas, E., Bell, T., Butler, J. H., Carpenter,
879    L. J., Jones, C. E., Harris, N. R. P., Hepach, H., Heumann, K. G., Hughes, C., Kuss, J., Kruger, K.,
880    Liss, P., Moore, R. M., Orlikowska, A., Raimund, S., Reeves, C. E., Reifenhauser, W., Robinson,
881    A. D., Schall, C., Tanhua, T., Tegtmeier, S., Turner, S., Wang, L., Wallace, D., Williams, J.,
882    Yamamoto, H., Yvon-Lewis, S., and Yokouchi, Y.: Global sea-to-air flux climatology for
883    bromoform, dibromomethane and methyl iodide, Atmospheric Chemistry and Physics, 13, 8915-
884    8934, 10.5194/acp-13-8915-2013, 2013.